Journal of Power Sources 204 (2012) 177–181

Contents lists available at SciVerse ScienceDirect

Journal of Power Sources

journal homepage: www.elsevier.com/locate/jpowsour

Short communication

New advanced cathode material: $LiMnPO_4$ encapsulated with $LiFePO_4$

K. Zaghib[a,*], M. Trudeau[a], A. Guerfi[a], J. Trottier[a], A. Mauger[b], R. Veillette[a], C.M. Julien[c]

[a] Energy Storage and Conversion, Hydro-Québec Research Institute, 1800 Boul. Lionel-Boulet, Varennes, Québec, Canada J3X 1S1
[b] Institut de Minéralogie et Physique de la Matière Condensée, Université Pierre et Marie Curie, Case courrier 115, 4 Place Jussieu, 75252 Paris Cedex 05, France
[c] Physicochimie des Electrolytes, Colloïdes et Sciences Analytiques (PECSA), Université Pierre et Marie Curie, Bat. F, 4 Place Jussieu, 57252 Paris Cedex 05, France

ARTICLE INFO

Article history:
Received 24 October 2011
Received in revised form
29 November 2011
Accepted 30 November 2011
Available online 9 December 2011

Keywords:
Lithium manganese phosphate
Cathode material
Encapsulation
Lithium-ion batteries

ABSTRACT

Coating the members of the olivine family $LiMPO_4$ with conductive carbon is difficult, excepted in the case M=Fe. To overcome this difficulty, we found possible to coat $LiMnPO_4$ with a thin layer of $LiFePO_4$ to take benefit of the catalytic reaction of Fe with C, so that a 3 nm-thick layer of carbon can be deposited at the surface of this composite. We find that the electrochemical properties of the carbon-coated $LiFePO_4$–$LiMnPO_4$ composite are improved with respect to the carbon-coated $LiMn_{2/3}Fe_{1/3}PO_4$ solid solution with comparable Fe/Mn ratio. Therefore, the use of a $LiFePO_4$ as a buffer layer between the high-density cathode element (like $LiMnPO_4$) and the carbon layer opens a new route to improve the performance of the olivine family as the active element of the cathode for Li-ion batteries.

1. Introduction

Li-ion batteries are emerging as one of the most promising technology for energy storage. To improve the overall battery performance, different materials are currently investigated. Among them, the olivine family is known to be promising as cathode element. In particular, $LiFePO_4$-batteries are already a growing part of the market, including for demanding applications such as electric and hybrid vehicles. First proposed by Padhi et al. [1], $LiFePO_4$ suffered from the fact that its electronic conductivity is small, but the coating of the particles with conductive carbon has solved this problem [2]. However, the relatively small voltage (3.4 V vs. Li^+/Li^0) limits the energy density. The other members $LiMPO_4$ of the olivine family with M=Mn, Co, Ni have a higher redox potential (4.1, 4.8 and 5.1 V vs. Li^+/Li^0, respectively), and thus higher theoretical energy densities. Since a voltage larger than 4.5 V still poses some problems of stability for various components of the batteries, attention has been focussed to $LiMnPO_4$. However, the electrochemical performance is very poor, for different reasons discussed elsewhere [3], unless the particle size is reduced to the order of 100 nm [4–7]. But even so, carbon coating is required, since this compound is even more resistive than $LiFePO_4$. Unfortunately, the deposit of conductive carbon on $LiMnPO_4$ is more difficult. The interaction between Fe and carbon [8] has been lost with the substitution of Fe by Mn. Additional reasons are discussed in the next section. Many efforts have been made to prepare C-$LiMnPO_4$ particles [9–14]. The price to obtain an initial discharge capacity in the range 130–140 mAh g^{-1} at C/10 rate was to immerse the $LiMnPO_4$ in important quantities of carbon, namely in the range 20 wt.% [15] to 30% [16,17]. However, the amount of carbon in a commercial lithium-ion battery should not excess few percents, in which case the capacity is smaller [18] and the material contains Li_3PO_4 impurity acting as an inert mass [19].

We report hereunder a different approach, which consists in coating the $LiMnPO_4$ particles with $LiFePO_4$. There has been an extensive research in the past to coat $LiCoO_2$ particles with metal oxides, reviewed in Ref. [20]. The coat aimed at a protection against the formation of a solid–electrolyte interface and Co dissolution. Indeed, the $LiFePO_4$ coating improved the cycling life of $LiCoO_2$ [21]. No such attempt, however, has been made on olivine compounds so far. In the present work, we report the effect of coating the $LiMnPO_4$ particles with $LiFePO_4$. After the particles have been coated with $LiFePO_4$, the composite particles are carbon-coated to assure a good conductivity.

It is essential to perform complete characterization of the structure and of the chemical nature of the different species present in the material at the nanometer level, in order to correctly understand the macroscopic properties of these nano-composite functionalized materials. In this work, we show the results of high-resolution structural and chemical analysis of this new electrode C-$LiFePO_4$–$LiMnPO_4$ composite, designed to improve the properties of lithium ion batteries. The high resolution characterization was done using a dedicated scanning transmission electron microscope (STEM), which allows for very fast energy-dispersive X-ray

* Corresponding author. Tel.: +1 450 652 8019; fax: +1 450 652 8424.
E-mail address: zaghib.karim@ireq.ca (K. Zaghib).

0378-7753/$ – see front matter © 2011 Elsevier B.V. All rights reserved.
doi:10.1016/j.jpowsour.2011.11.085

(EDX) elemental analysis with the real possibility of elemental mapping at the nanometer or even sub-nanometer level.

The electrochemical performance is reported for a product that contains 1/3 $LiFePO_4$ and 2/3 $LiMnPO_4$ in composition, and compared with that of a solid solution with the equivalent composition, i.e. $LiFe_{1/3}Mn_{2/3}PO_4$. The composite has a first charge capacity 116 mAh g^1 at low rate, and 65.5 mAh g^1 at 10C rate. The cycling at charge rate C/4 and discharge rate 1C for the solid solution shows that the reversible capacity is 119 mAh g^{-1} over 100 cycles. Under the same conditions, the results for the solid solution are 54.5, 23.3 and 55.7 mAh g^{-1}, respectively, which sizes the major improvement obtained for the composite.

2. Experimental details

Two different materials have been prepared. The new C-$LiFePO_4$-coated $LiMnPO_4$, to which we simply refer as the composite for simplicity, and the C-$LiMn_{2/3}Fe_{1/3}PO_4$ for comparison (both samples have the same proportion of Mn and Fe).

2.1. Synthesis of the composite

The whole synthesis process was performed under N_2 atmosphere. The water used in the synthesis process was demineralized and degassed. The synthesis procedure consists in several steps described hereunder.

Step 1: synthesis of $LiMnPO_4$ particles. A solute *A* is first obtained by dissolution of 4.62 g of $LiOH{\cdot}H_2O$ in 30 ml of water. A solute *B* is obtained by dissolution of 9.27 g of $Mn(NO_3)_2{\cdot}4H_2O$ in 50 ml of water. A solute C is obtained by dissolution of 9.27 g of an aqueous solution at 85% of H_3PO_4 in 10 ml of water. The solutes B and C are mixed together first. Then, the solute A is added gradually. The viscosity of the product increases wit the amount of A in the solution, and the final pH is 6.6. The resulting Mn concentration is 0.4 mole, and the Li/Mn/P elements are in the proportion 3/1/1. Then, this reactive medium is poured into a polytetrafluoroethylene (PTFE) vessel, put into a stainless steel chamber (Parr, volume = 325 ml), heated at 220 °C for 7 h. After cooling at room temperature, the powder is obtained by filtration, washed three times in distilled water, and dried at 90 °C during 12 h in N_2 atmosphere. After repeating twice the whole procedure, 12 g of $LiMnPO_4$ is obtained.

Step 2: coating with $LiFePO_4$. A solute D is obtained by dissolution of 308 g of $LiOH{\cdot}H_2O$ in 40 ml of water. A solute E is obtained by dissolution of 10 g of $FeSO_4{\cdot}7H_2O$ and 4.75 g of $(NH_4)_2HPO_4$ in 50 ml of water. The solute D is added progressively into E, and the final pH is 10.3. The product thus obtained is the precursor solution and the Li/Fe/P elements are in the ratio 2/1/1. Then, 10 g of $LiMnPO_4$ prepared in step 1 is added to this precursor solution. The reactive medium thus obtained is poured into a PTFE vessel and from now on, the process is the same as the one described in step one. At the end, 15.1 g of $LiFePO_4$-coated $LiMnPO_4$ is obtained.

Step 3: carbon-coating. The composite obtained at the end of step 2 has been mixed with a solution of lactose, the ratio lactose/composite being 1/10. This product has been heated at 400 °C for 1 h, then heated at 600 °C for 3 h. One difficulty met with $LiMnPO_4$ comes from the rapid degradation of the material and a heterogeneous carbon layer upon calcination at temperature T_{ca} above 650 °C [18]. Although the electric conductivity of the carbon layer increases fast with T_{ca} [22], the optimum temperature T_{ca} = 700 °C determined for $LiFePO_4$ [23] seems to be prohibited with $LiMnPO_4$. That is the reason why T_{ca} has been restricted to 600 °C in the present work.

2.2. Synthesis of the $LiMn_{2/3}Fe_{1/3}PO_4$

This material, synthesized to compare its electrochemical properties with those of the composite with the same ratio Mn/Fe, was prepared following the same procedure, since we wanted to obtain the same size distribution of the particles as in the composite samples. The only difference is that the solutes B and C were replaced by a solute obtained by dissolution of 3.33 g of $FeSO_4{\cdot}7H_2O$, 4.02 g of $MnSO_4{\cdot}H_2O$ and 4.75 g of NH_4HPO_4 in 50 ml of water. The carbon coating process was the same as the one used for the composite.

2.3. Apparatus

The characterization of the samples was done using a Hitachi HD-2700C dedicated STEM with a CEOS aberration corrector and a cold field-emission gun equipped with a newly designed silicon-drift detector (SDD) from Bruker, which offers over 10 times the solid angle of conventional energy-dispersive X-ray (EDX) detector. This dedicated STEM has demonstrated an image resolution of 78 pm in high angle annular dark field (HAADF). The electrochemical performances were tested with a cell in which the sample is the cathode, and the anode was Li metal. The electrolyte was a solution of 1 mol l^{-1} $LiPF_6$ in EC/DEC (50/50).

3. Results and discussion

The XRD spectrum of the C-$LiFePO_4$–$LiMnPO_4$ composite reported in Fig. 1 shows that the material is well crystallized in the olivine structure. Since the lattice parameters of $LiFePO_4$ and $LiMnPO_4$ are close, it is not possible to separate the peaks of each component at small angle, but they can be separated at high angle, so that both components are well crystallized. No extrinsic peak was detected. However, the XRD analysis does not tell us anything about the spatial distribution of $LiFePO_4$. The material is thus better characterized by electron microscopy. EDX spectra at different spots of the powder are shown in Fig. 2. The spectra show that the Mn peak intensity is larger than that of Fe, although the ratio of the peaks varies to some extent with the selected area. The integrated intensity of the EDX peaks modulated by the scattering efficiency of the different elements is consistent with the composition $LiFePO_4/LiMnPO_4$ in the ratio $0.33/0.66 \pm 0.02$.

The images of several particles representative of the sample are shown in Fig. 3. The particles are 0.1–0.2 μm in size. The maps of P is quite homogeneous across the particles. The same holds

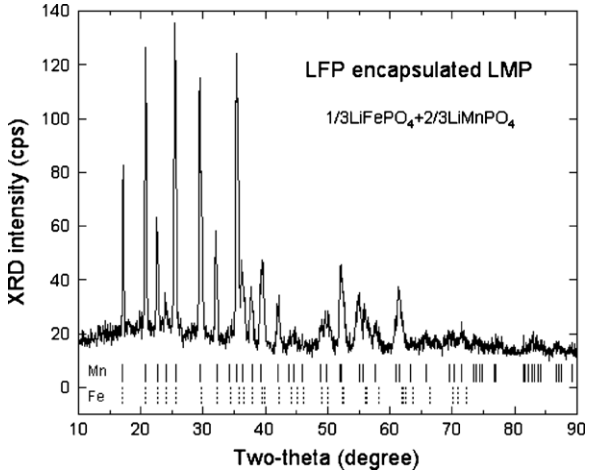

Fig. 1. X-ray diffraction pattern of the C-$LiFePO_4$–$LiMnPO_4$ composite. The positions of the XRD lines associated to the two components are identified by the bars below the spectrum.

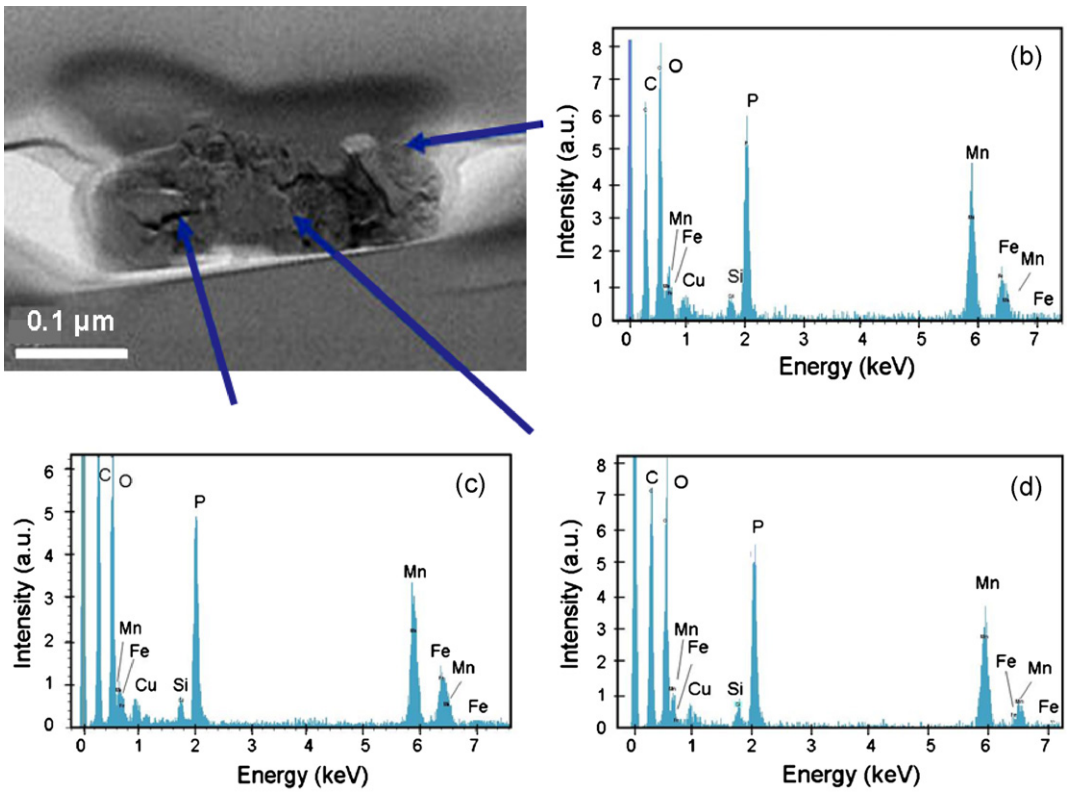

Fig. 2. EDX spectra at three spots show that both Mn and Fe in the analyzed areas with Mn peak intensity higher than Fe's one. On average, the relative concentration Mn:Fe is 2/3:1/3. (Cu and Si are from the sample support.)

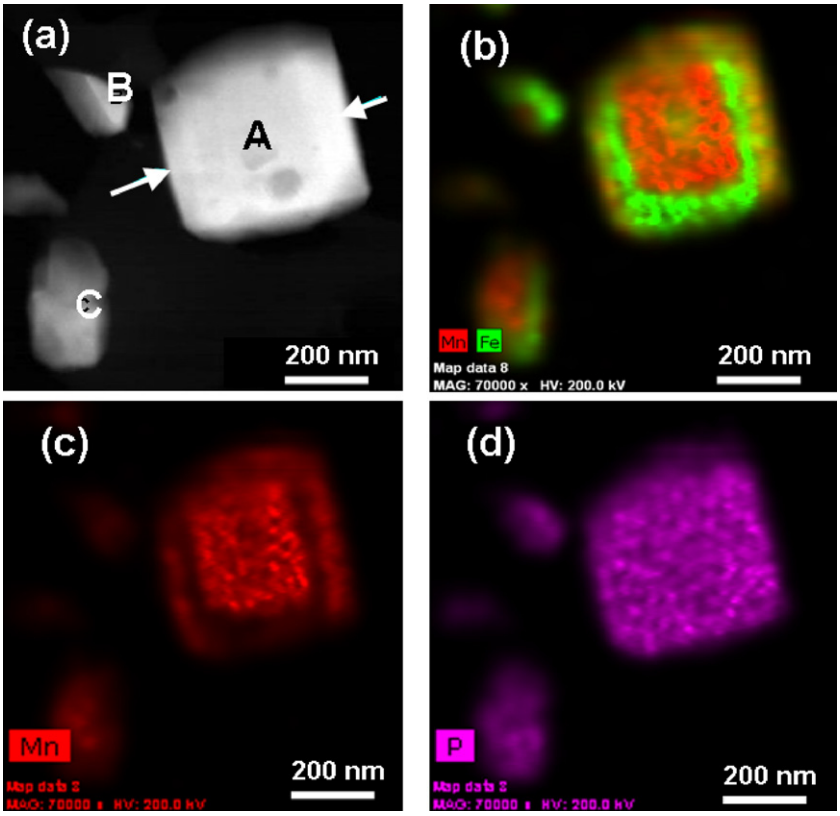

Fig. 3. Image of several particles of the composite (a), and EDX maps of the elements (b–d). The maps suggest that grain A has $LiMnPO_4$ at the center, with an outer layer of $LiFePO_4$ (two sides indicated by arrows in (b)). Grain D and B are mainly $LiFePO_4$. Grain C is partially covered by $LiFePO_4$ (left side).

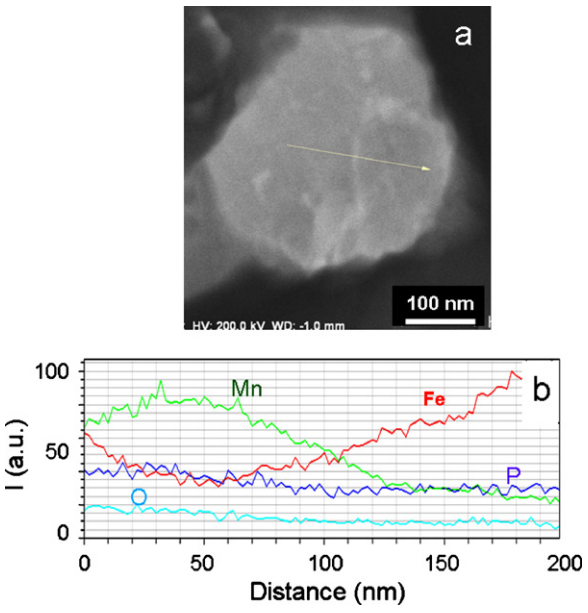

Fig. 4. (a) STEM image of a composite particle and (b) EDX line scan along the arrow in (a). The Fe content is minimized at the center of the grain and maximum at the boundary, while Mn content has the opposite trend, the P and O distributions are homogeneous. This suggests that $LiFePO_4$ forms a layer on the $LiMnPO_4$ core.

true for the oxygen element (not shown in the figure). The maps of most particles are like the particle named "A" in Fig. 3, with $LiMnPO_4$ in the center, coated with a layer of $LiFePO_4$. The thickness of the $LiFePO_4$ layer varies from 10 to several tens of nanometers. On another hand, the particle "C" is only partially covered with $LiFePO_4$. At last, there are also few particles (like "D" and "B" in Fig. 2) that are $LiFePO_4$ particles. To summarize the results illustrated by the structural analysis, $LiFePO_4$ forms a continuous layer that partly covers most of the $LiMnPO_4$ particles, but it also forms few small $LiFePO_4$ particles distributed sparsely. Another evidence of the coating of $LiMnPO_4$ by $LiFePO_4$ is illustrated in Fig. 4 showing a STEM image of a particle and the EDX line scan. The Fe content is minimum at the center and maximum at the surface, while the opposite holds true for the Mn content. The carbon coating on top of the $LiFePO_4$ layer is shown in Fig. 5, which also illustrates that the interface between $LiMnPO_4$ and $LiFePO_4$ is sharp. The strains at the

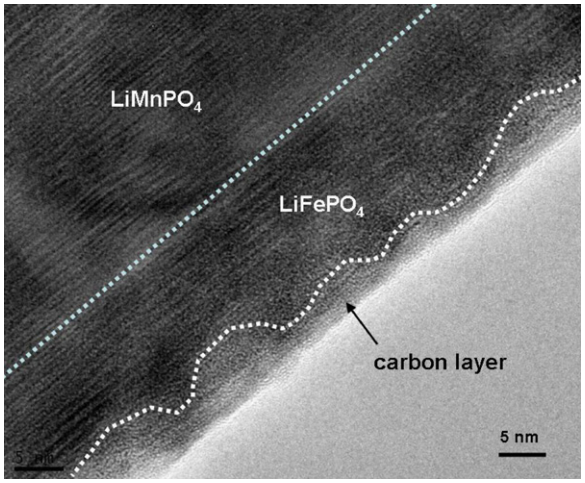

Fig. 5. TEM image near he surface of a particle of the composite showing the different layers. Note the interface between $LiMnPO_4$ and $LiFePO_4$ is sharp. The carbon layer is continuous, but irregular, as a consequence of the rather low calcination temperature 600 °C. The circle is here to point to a dislocation defect.

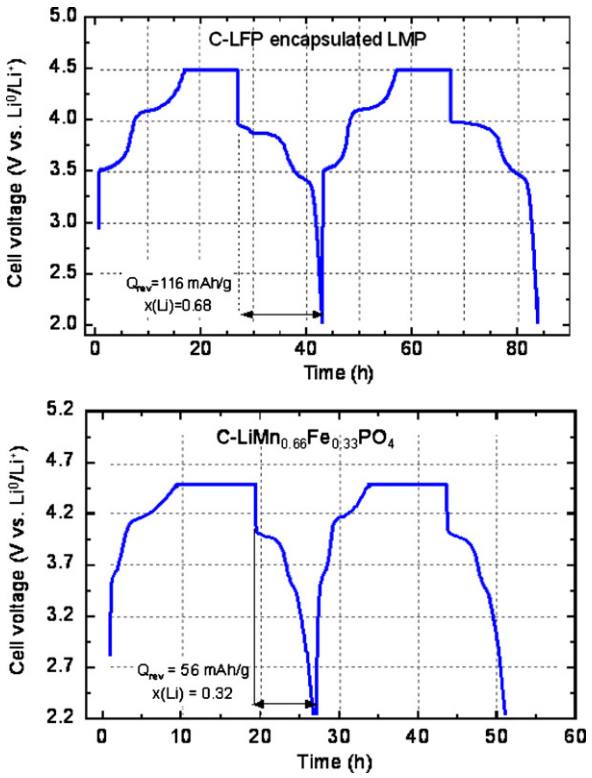

Fig. 6. Voltage as a function of time in charge/discharge conditions corresponding to theoretical rate C/24 for the composite C-$LiFePO_4$–$LiMnPO_4$ and $LiMn_{2/3}Fe_{1/3}PO_4$ for comparison.

interface between the two materials are accommodated by extended defects such as the dislocation outlined by the circle in the figure. On another hand, the $LiFePO_4$ layer is well crystallized. This result suggests that $LiFePO_4$ is deposited by some epitaxial effect on the well-crystallized surface of $LiMnPO_4$, since the free surface of $LiFePO_4$ at 600 °C is disordered [23]. The carbon layer is continuous, but with an irregular thickness. This is expected, since we have shown recently by in situ TEM experiments [23] that the uniform carbon coat of $LiFePO_4$ with a regular thickness requires a heating at $T_{ca} \geq 650$ K, which we avoided here to protect $LiMnPO_4$.

The electrochemical properties are illustrated in Fig. 6, showing the variation of the potential with time for the first two cycles. The current has been fixed to the value that would correspond to theoretical cycles at C/24 rate. Fig. 6 shows that the cycles only last 36 h each, because the capacity that could be obtained is smaller than theoretical. The flat part corresponds to the limit of 4.5 V imposed to the potential to protect the electrolyte. The first plateau observed at 3.5 V is characteristic of the Fe^{2+}/Fe^{3+} redox potential vs. Li in $LiFePO_4$. The next plateau at 4.0 V is characteristic of the Mn^{2+}/Mn^{3+} potential in $LiMnPO_4$, so that both components efficiently contribute to the electrochemical properties. We find that the capacity of the first charge is 119.3 mAh g^{-1} with a ratio discharge/charge (D/C) close to unity. This is still true in more drastic conditions shown in Fig. 7, when the cycles correspond to the charge rate C/4 and discharge rate 1C. The Ragone plot is shown in Fig. 8. At 10C, the delivered capacity is 65.5 mAh g^{-1}. For comparison, the results obtained on a sample $LiMn_{2/3}Fe_{1/3}PO_4$ are reported in the same figures for comparison. The capacity of the first charge is only 54.5 mAh g^{-1}, and the delivered capacity at 10C is only 23.3 mAh g^{-1}.

The $LiMnPO_4$ particles coated with $LiFePO_4$ and conductive carbon on top of it have then electrochemical properties that are much better than $LiMn_{2/3}Fe_{1/3}PO_4$, which illustrates the gain obtained

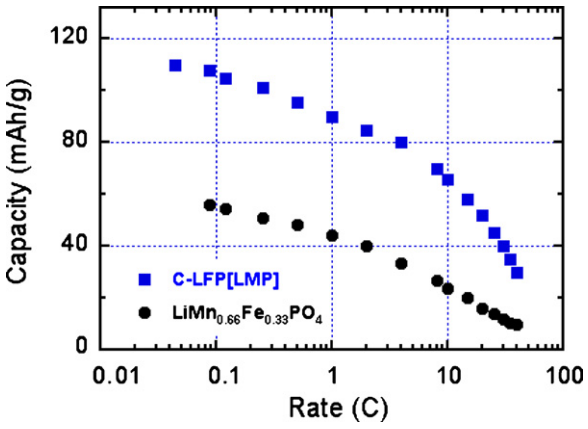

Fig. 7. Percentage of the capacity (left scale) and discharge over charge ratio D/C (right scale) as a function of the cycle number. In this experiment, the charge rate is C/4, and the discharge rate is 1C.

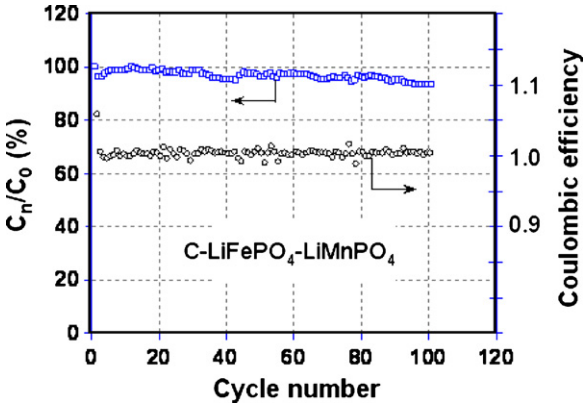

Fig. 8. Ragone plot for the C-$LiFePO_4$–$LiMnPO_4$ and $LiMn_{2/3}Fe_{1/3}PO_4$ samples for comparison.

with the composite over the alloy corresponding to the same composition. This is a remarkable result if we note that the $LiFePO_4$ layer has not been optimized yet, as it is continuous, but not uniform. As a consequence, part of $LiMnPO_4$ is not protected by $LiFePO_4$. We believe that efforts should now be focussed on the optimization of the synthesis parameters to improve the surface coverage. Actually, if a complete coating could be achieved, so that the $LiMnPO_4$ core would be completely protected, the calcination temperature might be increased to obtain a uniform coating of the composite with conductive carbon, achieved only at slightly higher temperatures than 600 °C used in this work [23]. Some prior works suggest that the temperature can be raised to 650 °C to achieve a uniform carbon coating of $LiMnPO_4$ without damaging the material [18]. In that case, the increase of T_{ca} to this value should result in an improvement of the electrochemical properties even if the coating of the $LiMnPO_4$ particles by $LiFePO_4$ would not be complete, because the carbon coating would be uniform [18]. We thus believe that our results should still be improved in the future. The important improvement that we have already obtained with the composite calcined at 600 °C only gives evidence that the $LiFePO_4$ coating, and thus the carbon coating on top of it, covers enough of the $LiFePO_4$ particles to percolate throughout the structure, and insure the electronic conductivity. The present work thus opens a new route to improve the electrochemical performance of the cathode elements of the olivine family.

4. Conclusion

We have presented a innovative cathode material in the form of composite particles. The core of the particles is $LiMnPO_4$, on which is deposited a $LiFePO_4$ film, the order of 10 nm-thick, with a carbon layer about 3 nm-thick on top of it. The $LiFePO_4$ film is homogenous, but does not fully cover the $LiMnPO_4$ yet, and the synthesis parameters have still to be optimized to reach this goal in the future. Nevertheless, the electrochemical properties are already significantly improved in terms of power density, ageing upon cycling and capacity with respect to the $LiMn_{2/3}Fe_{1/3}PO_4$ alloy with the same ratio Mn/Fe as in the composite. This result is attributable to the fact that the $LiFePO_4$ shell allows for the coating of the composite, while it is difficult to deposit the carbon at the surface of $LiMnPO_4$ at temperature small enough to avoid its decomposition. This carbon layer improves the electrical contact between the particles, and consequently the performance at high C-rate. In addition, the $LiFePO_4$ layer may avoid side reactions with the electrolyte, since the electrochemical properties do not degrade upon cycling, at least during the 100 first cycles that have been tested. The synthesis of composite particles of active elements of the olivine family is thus a promising route to improve the energy density of future Li-ion batteries, since both the $LiFePO_4$ and the $LiMnPO_4$ are active materials, and the composite takes benefit of the higher redox potential of Mn^{2+}/Mn^{3+} vs. Li^+/Li^0.

References

[1] A.K. Padhi, K.S. Nanjundaswamy, J.B. Goodenough, J. Electrochem. Soc. 144 (1997) 1188.
[2] N. Ravet, Y. Chouinard, J.F. Magnan, S. Besner, M. Gauthier, M. Armand, J. Power Sources 97–98 (2001) 503.
[3] M. Kopek, A. Yamada, G. Kobayashi, S. Nishimura, R. Kannoo, A. Mauger, F. Gendron, C.M. Julien, J. Power Sources 189 (2009) 1154.
[4] G. Arnold, J. Garche, R. Hemmer, S. Ströbele, C. Vogler, M. Wohlfahrt-Mehrens, J. Power Sources 119–121 (2003) 247.
[5] S.-Y. Chung, J.T. Bloking, Y.-M. Chiang, Nat. Mater. 1 (2002) 123.
[6] H. Huang, S.-C. Yin, L.F. Nazar, Electrochem. Solid State Lett. 4 (2001) A170.
[7] K. Zaghib, M. Dontigny, A. Guerfy, P. Charest, I. Rodrigues, A. Mauger, C.M. Julien, J. Power Sources 196 (2011) 3949.
[8] N. Ravet, M. Gauthier, K. Zaghib, J.B. Goodenough, A. Mauger, F. Gendron, C.M. Julien, Chem. Mater. 19 (2007) 2595.
[9] Y.S. Choi, S. Kim, S.S. Choi, J.S. Han, J.D. Kim, S.E. Jeon, B.H. Jung, Electrochim. Acta 50 (2004) 833.
[10] S. Kuroda, N. Tobori, M. Sakuraba, Y. Sato, J. Power Sources 119–121 (2003) 924.
[11] W. Xing, S.Z. Qiao, R.G. Ding, F. Li, G.Q. Lu, Z.F. Yan, H.M. Cheng, Carbon 44 (2006) 216.
[12] Q. Zhang, G. Peng, G. Wang, M. Qu, Z.L. Yu, Solid State Ionics 180 (2009) 698.
[13] Z. Bakenov, I. Taniguchi, J. Electrochem. Soc. 157 (2010) A430.
[14] Z. Bakenov, I. Taniguchi, Solid State Ionics 176 (2005) 1027.
[15] Z. Bakenov, I. Taniguchi, J. Power Sources 195 (2010) 7445.
[16] S.-M. Oh, H.-G. Jung, C.S. Yoon, S.-T. Myung, Z. Chen, K. Amine, Y.-K. Sun, J. Power Sources 196 (2011) 6924.
[17] S.-M. Oh, S.-W. Oh, C.-S. Yoon, B. Scrosati, K. Amine, Y.-K. Sun, Adv. Funct. Mater. 20 (2010) 3260.
[18] S.-M. Oh, S.W. Oh, S.-T. Myung, S.-M. Lee, Y.-K. Sun, J. Alloys Compd. 506 (2010) 372.
[19] P. Axmann, C. Stinner, M. Wolfahrt-Mehrens, A. Mauger, F. Gendron, C.M. Julien, Chem. Mater. 21 (2009) 1936.
[20] T.-F. Yi, J. Shu, Y. Wang, J. Xue, J. Meng, C.-B. Yue, R.-S. Zhu, Surf. Coat. Technol. 205 (2011) 3885.
[21] H. Wang, W.-D. Zhang, L.-Y. Zhu, M.-C. Chen, Solid State Ionics 178 (2007) 131.
[22] C.M. Julien, K. Zaghib, A. Mauger, M. Massot, A. Salah, M. Selmane, F. Gendron, J. Appl. Phys. 100 (2006) 63511.
[23] M.L. Trudeau, D. Laul, R. Veillette, A.M. Serventi, K. Zaghib, A. Mauger, C.M. Julien, J. Power Sources 196 (2011) 7383.